



Received 24 July 2024

Accepted 17 September 2024

Edited by W. T. A. Harrison, University of Aberdeen, United Kingdom

Keywords: 1-1'-binaphthyl derivative; non-spherical refinement; Hirshfeld surface analysis; crystal structure.

CCDC reference: 2384706

Supporting information: this article has supporting information at journals.iucr.org/e

Synthesis, non-spherical structure refinement and Hirshfeld surface analysis of racemic 2,2'-diisobutoxy-1,1'-binaphthalene

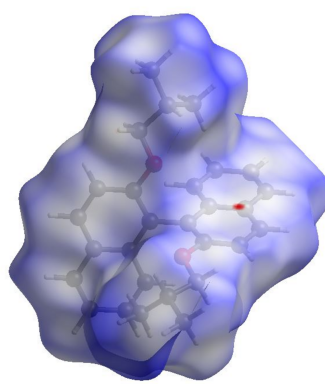
Pénayori Marie-Aimée Coulibaly,^a Eric Ziki,^{b*} Yvon Bibila Mayaya Bisseyou,^b Tchambaga Etienne Camara,^a Souleymane Coulibaly^a and Drissa Sissouma^a

^aLaboratoire de Constitution et de Réaction de la Matière, Equipe Synthèse Organique, UFR de Sciences des Structures de la Matière et Technologie, Université Félix Houphouët Boigny, 22 BP 582 Abidjan 22, Côte d'Ivoire, and ^bLaboratoire des Sciences de la Matière, de l'Environnement et de l'Energie Solaire, Equipe de Recherche de Cristallographie et Physique Moléculaire, Université Félix Houphouët-Boigny, 08 BP 582, Abidjan 22, Côte d'Ivoire. *Correspondence e-mail: eric.ziki@gmail.com

In the racemic title compound, $C_{28}H_{30}O_2$, the naphthyl ring systems subtend a dihedral angle of $68.59(1)^\circ$ and the molecular conformation is consolidated by a pair of intramolecular C—H $\cdots\pi$ contacts. The crystal packing features a weak C—H $\cdots\pi$ contact and van der Waals forces. A Hirshfeld surface analysis of the crystal structure reveals that the most significant contributions are from H \cdots H (73.2%) and C \cdots H/H \cdots C (21.2%) contacts.

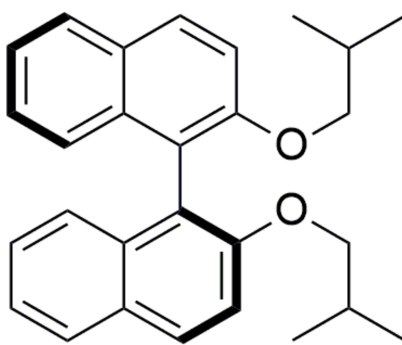
1. Chemical context

1-1'-Binaphthyl-based systems play an important role as ligands in the design of optically active materials (Tkachenko & Scheiner, 2019). They are also used for molecular recognition and asymmetric catalysis (Pu, 1998, 2024). The non-coplanar conformation of both naphthyl moieties coupled to their restricted rotation around the transannular covalent bond are the basis of their optical activity (chirality). Furthermore, it has been shown that, when substitutions are carried out at the 2,2'-positions of the 1-1'-binaphthyl system, the chiral conformation of the resulting derivative is very stable (Hall & Turner, 1955; Dixon *et al.*, 1971). Among these, 1-1'-bi-2-naphthol, $C_{20}H_{14}O_2$, known as BINOL, with local C_2 symmetry, has been used extensively in the production of chiral catalysts, dendrimers, molecular probes, metal-organic frameworks, covalent organic frameworks, *etc*. In addition, its hydroxyl functions can be functionalized to generate a wide range of 1-1'-binaphthyl derivatives. Many synthesis procedures of racemic BINOL have been developed using oxidizing agents such as Fe^{3+} , Cu^{2+} , Mn^{3+} , Ti^{2+} , Co^{3+} , Ag^{2+} or Mo^{5+} (Walvgogel, 2002; Doussot *et al.*, 2000; McKillop *et al.*, 1980; Budniak *et al.*, 2017) and pure enantiomers can be obtained from the their racemates *via* diastereoisomer derivatives and their resolution can be achieved by the formation of inclusion crystals with chiral host molecules (Hara *et al.*, 2002). Another strategy involves the deracemization of racemates with copper complexes of chiral amines (Bringmann *et al.*, 1990; Smrcina *et al.*, 1992) or by enzymatic hydrolysis of esters (Miyamo *et al.*, 1987; Kazlauskas *et al.*, 1989). Optically pure enantiomers can also be synthesized directly and several methods have been reported for this purpose (Chow *et al.*, 1996; Kawashima & Hirata, 1993; Wang *et al.*, 1995).



OPEN ACCESS

Published under a CC BY 4.0 licence



The racemic title compound, $C_{28}H_{30}O_2$ (I), is a 1-1'-bi-naphthal derivative obtained by the functionalization of BINOL at the hydroxyl positions. Herein, we report its synthesis, spectroscopic characterization and molecular geometry, determined from single-crystal X-ray diffraction analysis using a non-standard aspherical refinement, which combines quantum mechanical calculations and data from diffraction experiments into a single integrated tool (Jayatilaka & Dittrich, 2008; Capelli *et al.*, 2014; Kleemiss *et al.*, 2021). A Hirshfeld surface analysis (Spackman & Byrom, 1997; McKinnon *et al.*, 1998; McKinnon *et al.*, 2004) of the title compound was also performed.

2. Structural commentary

Compound (I) crystallizes in space group $P2_1/c$ as a racemate (Fig. 1). The molecular structure comprises two β -naphthyl isobutyl ether moieties linked by a $C1-C1'$ covalent bond whose length [1.4867 (3) Å] is in good agreement with the values reported for the same type of bond in related compounds (Allen & Bruno, 2010). Both ether units adopt extended conformations [$C2-O1-C11-C12 = -175.59(2)^\circ$;

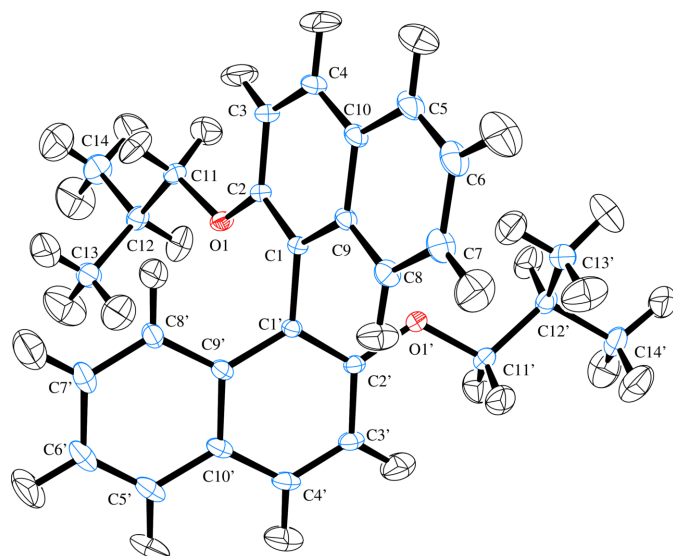


Figure 1

The molecular structure of (I) with displacement ellipsoids for all atoms including H drawn at the 50% probability level.

Table 1

Hydrogen-bond geometry (\AA , $^\circ$).

$D-H \cdots A$	$D-H$	$H \cdots A$	$D \cdots A$	$D-H \cdots A$
$C13-H13A \cdots Cg2$	1.091 (4)	2.998 (5)	4.0338 (4)	158.7 (3)
$C13'-H13E \cdots Cg1$	1.091 (5)	2.877 (5)	3.8615 (4)	150.1 (3)
$C13-H13C \cdots Cg2^i$	1.083 (5)	2.987 (5)	3.6455 (4)	119.6 (3)

Symmetry code: (i) $x, -y + \frac{3}{2}, z + \frac{1}{2}$.

$C2'-O1'-C11'-C12' = -175.12(2)^\circ]$ and the $C_{14}H_{15}O$ β -naphthyl isobutyl ether moieties exhibit very similar structural parameters with an alignment r.m.s.d. value of 0.023 Å (Fig. 2). The aromatic C–C bonds of the naphthal ring systems have values in the same range as those obtained by Rivera *et al.* (2017). The planes of the naphthal ring systems $C1-C10$ and $C1'-C10'$ (r.m.s. deviations of 0.013 Å and 0.037 Å, respectively) form a twist angle of $68.59(1)^\circ$ compared to $68.52(5)^\circ$ in BINOL (ref. date). The $C_{\text{ar}}-\text{O}$ and $C_{\text{alkyl}}-\text{O}$ ether bond lengths in (I) have comparable values to those found in related structures (Allen & Bruno, 2010). The molecular conformation of (I) is consolidated (Table 1) by intramolecular $C13'-H13E \cdots Cg1$ and $C13-H13A \cdots Cg2$ contacts, where $Cg1$ and $Cg2$ are the centroids of the $C5-C10$ and $C5'-C10'$ rings, respectively (Fig. 3, Table 1).

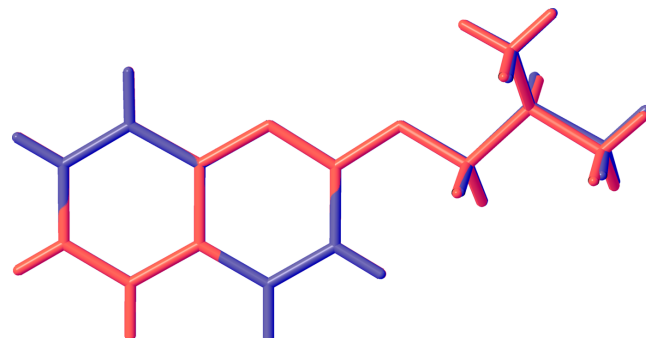


Figure 2

An overlay diagram of the β -naphthyl isobutyl ether moieties of (I).

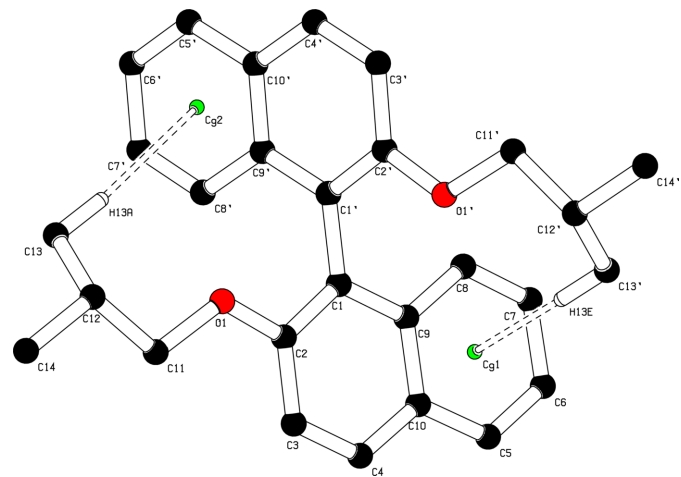
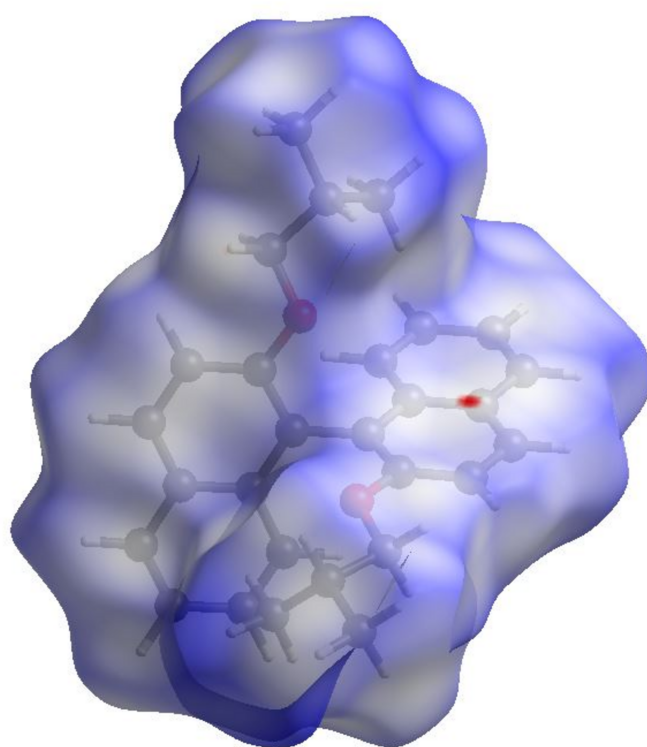


Figure 3

The intramolecular $C-\text{H} \cdots \pi$ interactions in (I), shown as double dotted lines with centroids as green spheres.

**Figure 4**

The three-dimensional Hirshfeld surface representation of (I) plotted over d_{norm} .

3. Supramolecular features

Although the molecule has two potential hydrogen-bond acceptor sites (atoms O1 and O2), no hydrogen bonding was found in this crystal structure. Indeed, the minimization of steric effects within the molecule gives rise to a structural

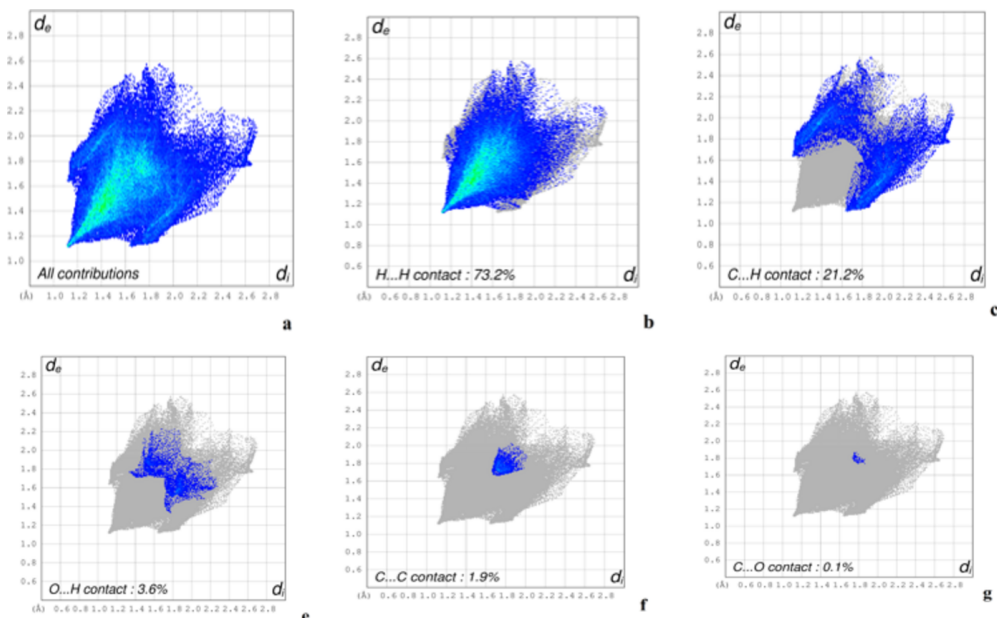
geometry whose intrinsic molecular and environmental parameters in the crystal would prevent the formation of hydrogen bonding. However, analysis using *PLATON* (Spek, 2020) reveals a C13—H13C···Cg2($x, \frac{3}{2} - y, \frac{1}{2} + z$) (Table 1). In addition, the packing displays several C—H···H—C intermolecular contacts ranging from 2.33 to 2.53 Å. Matta (2006) reported that these closed-shell intermolecular interactions exhibit energetic stability, potentials typical of bound systems and stable equilibrium geometries.

4. Database survey

A search of the Cambridge Structural Database (CSD version 5.45; Groom *et al.*, 2016) for compounds containing the 1-1'-binaphthyl system with an ether moiety linked at the 2,2' positions gave two hits [CSD refcodes PONTAO (Thoss *et al.*, 2009) and PONTAO01 (Maria *et al.*, 2017)], in which the asymmetric units contain two molecules.

5. Hirshfeld surface analysis

In order to quantify intermolecular interactions revealed by the *PLATON* analysis, Hirshfeld surface (HS) analysis was performed using *CrystalExplorer21.5* (Spackman *et al.*, 2021). Fig. 4 shows the three-dimensional HS of (I) mapped over d_{norm} on a scale ranging from −0.025 to 1.51 a.u. where the colour highlights the different intermolecular contacts: blue, white and red regions indicate contacts whose distances are almost equal, longer and shorter, respectively, than the sum of van der Waals radii. Fig. 5 displays the two-dimensional fingerprint plots of (d_i , d_e) points from all contacts contributing to the HS for all atoms. The H···H contacts are the most significant intermolecular interactions and contribute

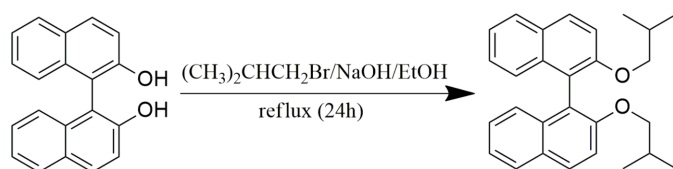
**Figure 5**

The two-dimensional fingerprint plots of (I) showing (a) the overall interactions and (b)–(f) those delineated into H···H, C···H/H···C, O···H/H···O, C···C and O···C/C···O contacts, respectively.

73.2% whilst C···H/H···C contacts, which correspond to H···π stacking interactions, contribute 21.2%. As expected, the H···O contacts make a very weak contribution to the crystal packing at 3.6% and the other contacts C···C (1.9%) and C···O/O···C (0.1%) have a negligible contribution.

6. Synthesis and crystallization

BINOL was produced according to the method described by McKillop *et al.* (1980). In a 50 ml flask equipped with a magnetic stirrer, 1 eq. (0.70 mmol, 0.20 g) of BINOL was dissolved in 10 ml of ethanol and 10 eq of sodium hydroxide were added. The mixture was refluxed for 1 h and 21 eq. (14.70 mmol, 1.58 ml) of 1-bromo-2-methylpropane were added, then heating was maintained for 24 h. Following CCM, at the end of the reaction, several extractions with ethyl acetate were performed and the organic phase was dried with NaSO₄, then concentrated under reduced pressure. The crude product was purified on a chromatographic silica gel column using hexane/ethyl acetate 90/10 as eluent. A chick yellow powder (60 mg, 21%) was obtained. Single crystals of (I) suitable for X-ray diffraction analysis were grown by slow evaporation from the mixed solvents of hexane and ethyl acetate at room temperature.



Chick yellow powder, yield = 47%, m.p = 387–389 K. ¹H NMR (500 MHz, CDCl₃) δ (ppm) 7.88 (*d*, *J* = 9.0 Hz, 2H, HAr), 7.81 (*dt*, *J* = 8.2, 1.1 Hz, 2H, HAr), 7.36 (*d*, *J* = 9.0 Hz, 2H, HAr), 7.26 (*ddd*, *J* = 8.1, 5.8, 2.1 Hz, 2H, HAr), 7.21–7.13 (*m*, 4H, HAr), 3.67 (*qd*, *J* = 8.8, 6.4 Hz, 4H, –CH₂–), 1.67 [*dh*, *J* = 13.2, 6.7 Hz, 2H, –CH–(CH₃)₂], 0.56 [*d*, *J* = 6.7 Hz, 6H, (CH₃)–CH–], 0.54 [*d*, *J* = 6.7 Hz, 6H, (CH₃)–CH–]. ¹³C NMR (126 MHz, CDCl₃) δ (ppm) 154.66, 134.44, 129.30, 129.09, 127.85, 126.10, 125.65, 123.42, 120.71, 115.62, 76.06, 28.45, 18.98.

7. Refinement details

The crystal structure of (I) was refined using *SHELXL* (Sheldrick, 2015b) with the standard independent atom model (IAM). Subsequently, this structural model was used as a starting point in a non-spherical refinement procedure. The computational wavefunctions were determined with the *ORCA* program (Neese *et al.*, 2020) using the DFT method at the PBE0/def2-TZVP level of theory. The non-spherical atomic form factors were calculated using *NoSphereA2* (Kleemiss *et al.*, 2021). Final refinements were performed with *OLEX2.refine* (Bourhis *et al.*, 2015). All atoms including H atoms were refined anisotropically. Crystal data, data collection and structure refinement details for the last least-squares refinement are summarized in Table 2. This process leads to

Table 2
Experimental details.

Crystal data	C ₂₈ H ₃₀ O ₂
Chemical formula	
M _r	398.55
Crystal system, space group	Monoclinic, <i>P2₁/c</i>
Temperature (K)	100
a, b, c (Å)	11.3889 (8), 15.6537 (11), 12.5193 (9)
β (°)	99.920 (2)
V (Å ³)	2198.6 (3)
Z	4
Radiation type	Mo <i>Kα</i>
μ (mm ⁻¹)	0.07
Crystal size (mm)	0.48 × 0.31 × 0.23
Data collection	
Diffractometer	Bruker D8 Venture
Absorption correction	Multi-scan (<i>SADABS</i> ; Krause <i>et al.</i> , 2015)
T _{min} , T _{max}	0.000, 0.000
No. of measured, independent and observed [I ≥ 2u(I)] reflections	215936, 17714, 14265
R _{int}	0.038
(sin θ/λ) _{max} (Å ⁻¹)	0.989
Refinement	
R[F ² > 2σ(F ²)], wR(F ²), S	0.023, 0.050, 1.08
No. of reflections	17714
No. of parameters	541
H-atom treatment	All H-atom parameters refined
Δρ _{max} , Δρ _{min} (e Å ⁻³)	0.20, -0.17

Computer programs: *APEX4* and *SAINT* (Bruker, 2019), *SHELXT2018/2* (Sheldrick, 2015a), *OLEX2.refine* (Bourhis *et al.*, 2015) and *OLEX2* (Dolomanov *et al.*, 2009).

improved precision of the geometrical parameters and more physically realistic C–H separations. For example, the refined C2–O1 bond length obtained here with the non-spherical model is 1.3622 (3) Å compared to 1.3652 (5) Å with IAM and the refined C2–O1–C11 bond angles are 118.315 (17)° (non-spherical) and 118.13 (3)° (IAM). For the background to non-spherical refinement, see Sanjuan-Szklarz *et al.* (2020) and Jha *et al.* (2023).

Acknowledgements

The authors thank the PMD2X X-ray diffraction facility (<https://crm2.univ-lorraine.fr/lab/fr/services/pmd2x>) of the Institut Jean Barriol, Université de Lorraine, for X-ray diffraction measurements and the AFRAMED project. CCDC is also thanked for providing access to the Cambridge Structural Database through the FAIRE program. The authors are very grateful to UNESCO, CNRS and the IUCr for their support to the AFRAMED project. The authors also thank PASRES for funding Coulibaly's thesis project. The authors pay a fitting tribute to Professor Ané Adjou of the Félix Houphouët-Boigny University, Supervisor of Coulibaly's PhD, who passed away in October 2023 before the thesis defence.

Funding information

Funding for this research was provided by: PASRES, a strategic support program for scientific research in Ivory Coast

(studentship No. 235/1st session of 2020 to Pénayori Marie-Aimée Coulibaly).

References

- Allen, F. H. & Bruno, I. J. (2010). *Acta Cryst. B* **66**, 380–386.
- Bourhis, L. J., Dolomanov, O. V., Gildea, R. J., Howard, J. A. K. & Puschmann, H. (2015). *Acta Cryst. A* **71**, 59–75.
- Bringmann, G., Walter, R. & Weirich, R. (1990). *Angew. Chem. Int. Ed. Engl.* **9**, 977–991.
- Bruker (2019). *APEX4* and *SAINT*. Bruker AXS Inc., Madison, Wisconsin, USA.
- Budniak, A. K., Masny, M., Prezelj, K., Grzeszkiewicz, M., Gawracyński, J., Dobrzycki, Ł., Cyrański, M. K., Koźmiński, W., Mazej, Z., Fijałkowski, K. J., Grochala, W. & Leszczyński, P. J. (2017). *New J. Chem.* **41**, 10742–10749.
- Capelli, S. C., Bürgi, H.-B., Dittrich, B., Grabowsky, S. & Jayatilaka, D. (2014). *IUCrJ*, **1**, 361–379.
- Chow, H. F., Wan, C. W. & Ng, M. K. (1996). *J. Org. Chem.* **61**, 8712–8714.
- Dixon, W., Harris, M. M. & Mazengo, R. Z. (1971). *J. Chem. Soc. B*, 775–778.
- Dolomanov, O. V., Bourhis, L. J., Gildea, R. J., Howard, J. A. K. & Puschmann, H. (2009). *J. Appl. Cryst.* **42**, 339–341.
- Doussot, J., Guy, A. & Ferroud, C. (2000). *Tetrahedron Lett.* **41**, 2545–2547.
- Groom, C. R., Bruno, I. J., Lightfoot, M. P. & Ward, S. C. (2016). *Acta Cryst. B* **72**, 171–179.
- Hall, D. M., Turner, E. E. & Howlett, K. E. (1955). *J. Chem. Soc.*, 1242–1251.
- Hara, T., Kawashima, H., Ishigooka, M., Kashiyama, M., Takanashi, S. & Hosokawa, Y. (2002). *Hepatogastroenterology*, **49**, 561–563.
- Jayatilaka, D. & Dittrich, B. (2008). *Acta Cryst. A* **64**, 383–393.
- Jha, K. K., Kleemiss, F., Chodkiewicz, M. L. & Dominiak, P. M. (2023). *J. Appl. Cryst.* **56**, 116–127.
- Kawashima, M. & Hirata, R. (1993). *Bull. Chem. Soc. Jpn.* **66**, 2002–2005.
- Kazlauskas, R. J. (1989). *J. Am. Chem. Soc.* **111**, 4953–4959.
- Kleemiss, F., Dolomanov, O. V., Bodensteiner, M., Peyerimhoff, N., Midgley, L., Bourhis, L. J., Genoni, A., Malaspina, L. A., Jayatilaka, D., Spencer, J. L., White, F., Grundkötter-Stock, B., Steinhauer, S., Lentz, D., Puschmann, H. & Grabowsky, S. (2021). *Chem. Sci.* **12**, 1675–1692.
- Krause, L., Herbst-Irmer, R., Sheldrick, G. M. & Stalke, D. (2015). *J. Appl. Cryst.* **48**, 3–10.
- Maria, T. M. R., Marins, F. A., Costa, J. B. S., Silva, M. R., Carrilho, R. M. B., Monteiro, C. J. P., Pereira, M. M. & Eusébio, M. E. S. (2017). *Thermochim. Acta*, **648**, 32–43.
- Matta, C. F. (2006). *Hydrogen Bonding – New Insights*, edited by S. Grabowski, pp. 337–375. Dordrecht: Springer.
- McKillop, A., Turrell, A. G., Young, D. W. & Taylor, E. C. (1980). *J. Am. Chem. Soc.* **102**, 6504–6512.
- McKinnon, J. J., Mitchell, A. S. & Spackman, M. A. (1998). *Chem. Eur. J.* **4**, 2136–2141.
- McKinnon, J. J., Spackman, M. A. & Mitchell, A. S. (2004). *Acta Cryst. B* **60**, 627–668.
- Miyano, T. & Beukes, N. J. (1987). *Econ. Geol.* **82**, 706–718.
- Neese, F., Wennmohs, F., Becker, U. & Riplinge, C. (2020). *J. Chem. Phys.* **152**, 224108.
- Pu, L. (1998). *Chem. Rev.* **98**, 2405–2494.
- Pu, L. (2024). *Chem. Rev.* **124**, 6643–6689.
- Rivera, A., Cepeda-Santamaría, J. E., Ríos-Motta, J. & Bolte, M. (2017). *Acta Cryst. E* **73**, 832–834.
- Sanjuan-Szklarz, W. F., Woińska, M., Domagała, S., Dominiak, P. M., Grabowsky, S., Jayatilaka, D., Gutmann, M. & Woźniak, K. (2020). *IUCrJ*, **7**, 920–933.
- Sheldrick, G. M. (2015a). *Acta Cryst. A* **71**, 3–8.
- Sheldrick, G. M. (2015b). *Acta Cryst. C* **71**, 3–8.
- Smrcina, M., Lorenc, M., Hanus, V., Sedmera, P. & Kocovsky, P. (1992). *J. Org. Chem.* **57**, 1917–1920.
- Spackman, M. A. & Byrom, P. G. G. (1997). *Chem. Phys. Lett.* **267**, 215–220.
- Spackman, P. R., Turner, M. J., McKinnon, J. J., Wolff, S. K., Grimwood, D. J., Jayatilaka, D. & Spackman, M. A. (2021). *J. Appl. Cryst.* **54**, 1006–1011.
- Spek, A. L. (2020). *Acta Cryst. E* **76**, 1–11.
- Thoss, M., Seidel, R. W. & Feigel, M. (2009). *Acta Cryst. E* **65**, o243.
- Tkachenko, N. V. & Scheiner, S. (2019). *ACS Omega*, **4**, 6044–6049.
- Waldvogel, S. L. (2002). *Synlett*, **4**, 622–624.
- Wang, M., Liu, S. Z., Liu, J. & Hu, B. F. (1995). *J. Org. Chem.* **60**, 7364–7365.

supporting information

Acta Cryst. (2024). E80, 1044-1048 [https://doi.org/10.1107/S2056989024009101]

Synthesis, non-spherical structure refinement and Hirshfeld surface analysis of racemic 2,2'-diisobutoxy-1,1'-binaphthalene

Pénayori Marie-Aimée Coulibaly, Eric Ziki, Yvon Bibila Mayaya Bisseyou, Tchambaga Etienne Camara, Souleymane Coulibaly and Drissa Sissouma

Computing details

2,2'-Diisobutoxy-1,1'-binaphthalene

Crystal data

C₂₈H₃₆O₂
 $M_r = 398.55$
Monoclinic, $P2_1/c$
 $a = 11.3889$ (8) Å
 $b = 15.6537$ (11) Å
 $c = 12.5193$ (9) Å
 $\beta = 99.920$ (2)°
 $V = 2198.6$ (3) Å³
 $Z = 4$
 $F(000) = 856.478$

$D_x = 1.204$ Mg m⁻³
Melting point: 389 K
Mo $K\alpha$ radiation, $\lambda = 0.71073$ Å
Cell parameters from 17714 reflections
 $\theta = 3.0\text{--}44.7^\circ$
 $\mu = 0.07$ mm⁻¹
 $T = 100$ K
Prism, colourless
0.48 × 0.31 × 0.23 mm

Data collection

Bruker D8 Venture
diffractometer
Radiation source: fine-focus sealed tube
Mirror monochromator
 φ and ω scan
Absorption correction: multi-scan
(SADABS; Krause *et al.*, 2015)
 $T_{\min} = 0.000$, $T_{\max} = 0.000$

215936 measured reflections
17714 independent reflections
14265 reflections with $I \geq 2u(I)$
 $R_{\text{int}} = 0.038$
 $\theta_{\max} = 44.7^\circ$, $\theta_{\min} = 3.0^\circ$
 $h = -22\text{--}22$
 $k = -30\text{--}30$
 $l = -24\text{--}24$

Refinement

Refinement on F^2
Least-squares matrix: full
 $R[F^2 > 2\sigma(F^2)] = 0.023$
 $wR(F^2) = 0.050$
 $S = 1.08$
17714 reflections
541 parameters
0 restraints
0 constraints

Primary atom site location: structure-invariant direct methods
Secondary atom site location: structure-invariant direct methods
Hydrogen site location: difference Fourier map
All H-atom parameters refined
 $w = 1/[\sigma^2(F_o^2) + (0.0137P)^2 + 0.0711P]$
where $P = (F_o^2 + 2F_c^2)/3$
 $(\Delta/\sigma)_{\max} = 0.002$
 $\Delta\rho_{\max} = 0.20$ e Å⁻³
 $\Delta\rho_{\min} = -0.17$ e Å⁻³

Fractional atomic coordinates and isotropic or equivalent isotropic displacement parameters (\AA^2)

	<i>x</i>	<i>y</i>	<i>z</i>	$U_{\text{iso}}^*/U_{\text{eq}}$
O1'	0.776199 (14)	0.498356 (11)	0.341745 (13)	0.01666 (3)
O1	0.734447 (14)	0.575536 (12)	0.638617 (13)	0.01737 (3)
C13'	0.59639 (2)	0.44710 (2)	0.15859 (2)	0.02417 (4)
C12'	0.70148 (2)	0.391771 (15)	0.210094 (18)	0.01879 (4)
C11'	0.80870 (2)	0.444976 (15)	0.259094 (18)	0.01713 (3)
C2'	0.857985 (17)	0.555997 (14)	0.390229 (16)	0.01385 (3)
C1'	0.816020 (16)	0.618843 (13)	0.452436 (15)	0.01271 (3)
C1	0.686874 (16)	0.621349 (13)	0.458654 (16)	0.01309 (3)
C2	0.648288 (17)	0.598891 (14)	0.554230 (17)	0.01449 (3)
C11	0.70253 (2)	0.567336 (16)	0.743665 (18)	0.01806 (4)
C12	0.81506 (2)	0.547883 (16)	0.824239 (18)	0.01962 (4)
C13	0.90482 (2)	0.62078 (2)	0.83150 (2)	0.02380 (4)
C14	0.78109 (3)	0.52831 (2)	0.93444 (2)	0.03137 (6)
C3	0.525397 (19)	0.598393 (16)	0.56113 (2)	0.01904 (4)
C4	0.442362 (19)	0.617508 (17)	0.47119 (2)	0.02111 (4)
C10	0.477288 (18)	0.639919 (15)	0.37163 (2)	0.01831 (4)
C9	0.601102 (18)	0.643888 (14)	0.366043 (17)	0.01499 (3)
C14'	0.74018 (3)	0.331031 (18)	0.12705 (2)	0.02435 (5)
C3'	0.980012 (19)	0.551723 (16)	0.380747 (18)	0.01786 (3)
C4'	1.059045 (19)	0.609785 (17)	0.43474 (2)	0.01970 (4)
C10'	1.020820 (18)	0.674390 (15)	0.500151 (18)	0.01737 (4)
C5'	1.10225 (2)	0.733859 (18)	0.55771 (2)	0.02357 (5)
C6'	1.06387 (3)	0.796215 (18)	0.62076 (2)	0.02631 (5)
C7'	0.94151 (3)	0.801770 (17)	0.62857 (2)	0.02385 (5)
C8'	0.86073 (2)	0.744848 (15)	0.574119 (19)	0.01854 (4)
C9'	0.897770 (17)	0.679042 (14)	0.508850 (16)	0.01448 (3)
C8	0.63491 (2)	0.670193 (16)	0.266644 (19)	0.01898 (4)
C7	0.55041 (2)	0.688558 (18)	0.17723 (2)	0.02395 (5)
C6	0.42742 (2)	0.681410 (19)	0.18200 (2)	0.02650 (5)
C5	0.39219 (2)	0.658060 (18)	0.27738 (2)	0.02444 (5)
H13D	0.6189 (4)	0.4843 (3)	0.0920 (4)	0.0446 (13)
H13E	0.5691 (4)	0.4921 (3)	0.2162 (4)	0.0384 (12)
H13F	0.5196 (4)	0.4074 (4)	0.1267 (4)	0.0510 (15)
H12'	0.6746 (4)	0.3538 (3)	0.2761 (3)	0.0326 (11)
H11C	0.8815 (4)	0.4033 (3)	0.2933 (4)	0.0337 (11)
H11D	0.8373 (4)	0.4850 (3)	0.1965 (3)	0.0306 (10)
H11A	0.6380 (4)	0.5162 (3)	0.7433 (4)	0.0360 (11)
H11B	0.6621 (4)	0.6265 (3)	0.7650 (3)	0.0355 (11)
H12	0.8545 (4)	0.4902 (3)	0.7947 (4)	0.0343 (11)
H13A	0.9295 (4)	0.6347 (3)	0.7529 (4)	0.0387 (12)
H13B	0.9853 (5)	0.6062 (4)	0.8885 (4)	0.0524 (15)
H13C	0.8669 (5)	0.6788 (3)	0.8581 (4)	0.0472 (14)
H14A	0.7414 (5)	0.5840 (4)	0.9646 (4)	0.0519 (15)
H14B	0.8591 (5)	0.5115 (4)	0.9937 (4)	0.0610 (17)
H14C	0.7172 (5)	0.4763 (4)	0.9293 (4)	0.0532 (15)

H3	0.4960 (4)	0.5800 (3)	0.6352 (4)	0.0368 (12)
H4	0.3491 (4)	0.6135 (3)	0.4759 (4)	0.0402 (12)
H14D	0.6658 (4)	0.2919 (3)	0.0891 (4)	0.0437 (13)
H14E	0.8111 (5)	0.2894 (3)	0.1636 (4)	0.0430 (13)
H14F	0.7714 (5)	0.3666 (3)	0.0630 (4)	0.0430 (13)
H3'	1.0126 (4)	0.5020 (3)	0.3349 (4)	0.0362 (11)
H4'	1.1523 (4)	0.6049 (3)	0.4296 (4)	0.0378 (12)
H5'	1.1953 (4)	0.7284 (3)	0.5514 (4)	0.0402 (12)
H6'	1.1258 (4)	0.8434 (3)	0.6632 (4)	0.0470 (14)
H7'	0.9117 (4)	0.8505 (3)	0.6778 (4)	0.0439 (13)
H8'	0.7674 (4)	0.7488 (3)	0.5805 (4)	0.0316 (11)
H8	0.7285 (4)	0.6756 (3)	0.2629 (3)	0.0335 (11)
H7	0.5776 (4)	0.7082 (3)	0.1026 (4)	0.0428 (13)
H6	0.3615 (4)	0.6941 (3)	0.1094 (4)	0.0448 (13)
H5	0.2992 (4)	0.6533 (3)	0.2823 (4)	0.0424 (13)

Atomic displacement parameters (\AA^2)

	U^{11}	U^{22}	U^{33}	U^{12}	U^{13}	U^{23}
O1'	0.01473 (6)	0.01960 (7)	0.01643 (6)	-0.00056 (5)	0.00487 (5)	-0.00336 (5)
O1	0.01438 (6)	0.02456 (8)	0.01393 (6)	0.00018 (5)	0.00453 (4)	0.00063 (5)
C13'	0.02086 (10)	0.03031 (12)	0.02154 (10)	-0.00184 (9)	0.00422 (8)	-0.00185 (9)
C12'	0.02491 (9)	0.01793 (9)	0.01485 (7)	-0.00341 (7)	0.00716 (7)	-0.00102 (6)
C11'	0.01920 (8)	0.01764 (8)	0.01564 (7)	0.00106 (7)	0.00607 (6)	-0.00095 (6)
C2'	0.01112 (6)	0.01761 (8)	0.01319 (6)	0.00082 (5)	0.00311 (5)	0.00077 (6)
C1'	0.01002 (6)	0.01598 (7)	0.01205 (6)	-0.00073 (5)	0.00165 (5)	0.00026 (5)
C1	0.00996 (6)	0.01569 (7)	0.01349 (6)	-0.00009 (5)	0.00166 (5)	-0.00110 (5)
C2	0.01134 (6)	0.01750 (8)	0.01524 (7)	-0.00087 (6)	0.00397 (5)	-0.00182 (6)
C11	0.01926 (8)	0.02077 (9)	0.01563 (7)	-0.00217 (7)	0.00720 (6)	0.00007 (6)
C12	0.02480 (10)	0.02033 (9)	0.01447 (7)	-0.00012 (7)	0.00543 (7)	0.00196 (7)
C13	0.02319 (10)	0.02987 (12)	0.01826 (9)	-0.00493 (9)	0.00332 (8)	0.00032 (8)
C14	0.04086 (16)	0.03786 (16)	0.01659 (9)	-0.00750 (13)	0.00833 (10)	0.00571 (10)
C3	0.01227 (7)	0.02384 (10)	0.02220 (9)	-0.00155 (6)	0.00635 (6)	-0.00351 (7)
C4	0.01030 (7)	0.02574 (10)	0.02732 (10)	-0.00002 (7)	0.00334 (7)	-0.00593 (8)
C10	0.01116 (7)	0.01935 (9)	0.02290 (9)	0.00211 (6)	-0.00134 (6)	-0.00484 (7)
C9	0.01172 (6)	0.01579 (8)	0.01639 (7)	0.00122 (5)	-0.00054 (5)	-0.00140 (6)
C14'	0.03660 (13)	0.01943 (10)	0.01878 (9)	-0.00291 (9)	0.00972 (9)	-0.00368 (8)
C3'	0.01218 (7)	0.02384 (10)	0.01839 (8)	0.00213 (6)	0.00501 (6)	0.00207 (7)
C4'	0.01049 (7)	0.02758 (11)	0.02121 (9)	-0.00055 (7)	0.00324 (6)	0.00521 (8)
C10'	0.01166 (7)	0.02219 (9)	0.01729 (8)	-0.00383 (6)	-0.00025 (6)	0.00516 (7)
C5'	0.01586 (8)	0.02704 (11)	0.02524 (10)	-0.00856 (8)	-0.00369 (7)	0.00664 (8)
C6'	0.02446 (11)	0.02484 (11)	0.02592 (11)	-0.01121 (9)	-0.00610 (8)	0.00256 (9)
C7'	0.02753 (11)	0.02049 (10)	0.02134 (9)	-0.00791 (8)	-0.00194 (8)	-0.00221 (8)
C8'	0.01907 (8)	0.01821 (9)	0.01760 (8)	-0.00435 (7)	0.00107 (6)	-0.00208 (6)
C9'	0.01218 (6)	0.01710 (8)	0.01350 (7)	-0.00279 (6)	0.00037 (5)	0.00179 (6)
C8	0.01749 (8)	0.02077 (9)	0.01702 (8)	0.00143 (7)	-0.00166 (6)	0.00284 (7)
C7	0.02476 (10)	0.02396 (10)	0.01983 (9)	0.00367 (8)	-0.00547 (8)	0.00346 (8)
C6	0.02236 (10)	0.02659 (11)	0.02585 (11)	0.00696 (8)	-0.00914 (8)	-0.00190 (9)

C5	0.01440 (8)	0.02673 (11)	0.02878 (11)	0.00514 (7)	-0.00592 (8)	-0.00621 (9)
H13D	0.043 (3)	0.049 (3)	0.044 (3)	0.013 (3)	0.012 (2)	0.014 (3)
H13E	0.035 (3)	0.044 (3)	0.038 (3)	0.003 (2)	0.009 (2)	-0.004 (2)
H13F	0.035 (3)	0.061 (4)	0.055 (4)	-0.010 (3)	0.000 (3)	-0.014 (3)
H12'	0.046 (3)	0.031 (3)	0.023 (2)	-0.009 (2)	0.012 (2)	-0.0006 (19)
H11C	0.033 (3)	0.035 (3)	0.034 (3)	0.006 (2)	0.006 (2)	-0.005 (2)
H11D	0.034 (3)	0.033 (2)	0.028 (2)	-0.008 (2)	0.012 (2)	-0.003 (2)
H11A	0.038 (3)	0.042 (3)	0.030 (3)	-0.012 (2)	0.011 (2)	0.000 (2)
H11B	0.040 (3)	0.041 (3)	0.027 (2)	0.008 (2)	0.010 (2)	-0.002 (2)
H12	0.046 (3)	0.029 (3)	0.028 (3)	0.006 (2)	0.006 (2)	0.001 (2)
H13A	0.039 (3)	0.049 (3)	0.030 (3)	-0.009 (2)	0.011 (2)	0.003 (2)
H13B	0.041 (3)	0.072 (4)	0.039 (3)	-0.012 (3)	-0.008 (2)	0.012 (3)
H13C	0.047 (3)	0.042 (3)	0.054 (3)	-0.012 (3)	0.014 (3)	-0.011 (3)
H14A	0.063 (4)	0.065 (4)	0.032 (3)	-0.008 (3)	0.021 (3)	-0.002 (3)
H14B	0.061 (4)	0.093 (5)	0.025 (3)	-0.006 (4)	-0.001 (3)	0.018 (3)
H14C	0.069 (4)	0.060 (4)	0.034 (3)	-0.025 (3)	0.016 (3)	0.011 (3)
H3	0.023 (2)	0.053 (3)	0.037 (3)	-0.002 (2)	0.011 (2)	-0.001 (2)
H4	0.022 (2)	0.056 (3)	0.044 (3)	0.004 (2)	0.007 (2)	-0.006 (3)
H14D	0.051 (3)	0.046 (3)	0.037 (3)	-0.014 (3)	0.017 (2)	-0.019 (2)
H14E	0.060 (3)	0.034 (3)	0.037 (3)	0.007 (3)	0.014 (3)	-0.004 (2)
H14F	0.061 (4)	0.041 (3)	0.032 (3)	-0.005 (3)	0.023 (3)	-0.004 (2)
H3'	0.026 (2)	0.040 (3)	0.045 (3)	0.003 (2)	0.014 (2)	-0.002 (2)
H4'	0.023 (2)	0.047 (3)	0.043 (3)	0.000 (2)	0.006 (2)	0.002 (2)
H5'	0.024 (2)	0.042 (3)	0.052 (3)	-0.013 (2)	0.001 (2)	0.003 (3)
H6'	0.033 (3)	0.057 (3)	0.045 (3)	-0.016 (3)	-0.008 (2)	-0.012 (3)
H7'	0.039 (3)	0.043 (3)	0.048 (3)	-0.013 (2)	0.003 (2)	-0.009 (3)
H8'	0.032 (2)	0.027 (2)	0.036 (3)	-0.002 (2)	0.005 (2)	-0.012 (2)
H8	0.031 (2)	0.045 (3)	0.024 (2)	0.004 (2)	0.0031 (19)	0.013 (2)
H7	0.045 (3)	0.048 (3)	0.030 (3)	0.006 (3)	-0.007 (2)	0.011 (2)
H6	0.032 (3)	0.050 (3)	0.046 (3)	0.011 (2)	-0.011 (2)	0.008 (3)
H5	0.026 (3)	0.056 (3)	0.041 (3)	0.003 (2)	-0.005 (2)	-0.006 (3)

Geometric parameters (\AA , $^{\circ}$)

O1'—C11'	1.4276 (3)	C3—C4	1.3729 (4)
O1'—C2'	1.3621 (3)	C3—H3	1.077 (4)
O1—C2	1.3622 (3)	C4—C10	1.4162 (4)
O1—C11	1.4293 (3)	C4—H4	1.075 (4)
C13'—C12'	1.5272 (4)	C10—C9	1.4252 (3)
C13'—H13D	1.083 (5)	C10—C5	1.4206 (3)
C13'—H13E	1.091 (5)	C9—C8	1.4253 (3)
C13'—H13F	1.091 (5)	C14'—H14D	1.086 (5)
C12'—C11'	1.5176 (3)	C14'—H14E	1.076 (5)
C12'—C14'	1.5287 (4)	C14'—H14F	1.086 (5)
C12'—H12'	1.103 (4)	C3'—C4'	1.3724 (4)
C11'—H11C	1.084 (4)	C3'—H3'	1.071 (4)
C11'—H11D	1.096 (4)	C4'—C10'	1.4162 (4)
C2'—C1'	1.3896 (3)	C4'—H4'	1.078 (4)

C2'—C3'	1.4166 (3)	C10'—C5'	1.4197 (3)
C1'—C1	1.4867 (3)	C10'—C9'	1.4261 (3)
C1'—C9'	1.4238 (3)	C5'—C6'	1.3733 (5)
C1—C2	1.3891 (3)	C5'—H5'	1.080 (4)
C1—C9	1.4258 (3)	C6'—C7'	1.4163 (4)
C2—C3	1.4170 (3)	C6'—H6'	1.093 (4)
C11—C12	1.5190 (4)	C7'—C8'	1.3744 (3)
C11—H11A	1.086 (4)	C7'—H7'	1.073 (5)
C11—H11B	1.088 (4)	C8'—C9'	1.4232 (3)
C12—C13	1.5243 (4)	C8'—H8'	1.081 (4)
C12—C14	1.5268 (4)	C8—C7	1.3750 (3)
C12—H12	1.101 (4)	C8—H8	1.078 (4)
C13—H13A	1.091 (4)	C7—C6	1.4167 (4)
C13—H13B	1.085 (5)	C7—H7	1.078 (5)
C13—H13C	1.083 (5)	C6—C5	1.3732 (5)
C14—H14A	1.079 (6)	C6—H6	1.093 (4)
C14—H14B	1.088 (5)	C5—H5	1.074 (5)
C14—H14C	1.086 (5)		
C2'—O1'—C11'	117.900 (17)	H14C—C14—H14B	108.6 (4)
C11—O1—C2	118.315 (17)	C4—C3—C2	119.79 (2)
H13D—C13'—C12'	110.9 (3)	H3—C3—C2	120.7 (2)
H13E—C13'—C12'	112.2 (3)	H3—C3—C4	119.4 (2)
H13E—C13'—H13D	107.1 (4)	C10—C4—C3	121.17 (2)
H13F—C13'—C12'	110.6 (3)	H4—C4—C3	119.3 (3)
H13F—C13'—H13D	107.8 (4)	H4—C4—C10	119.5 (3)
H13F—C13'—H13E	107.9 (4)	C9—C10—C4	118.97 (2)
C11'—C12'—C13'	112.14 (2)	C5—C10—C4	121.71 (2)
C14'—C12'—C13'	111.25 (2)	C5—C10—C9	119.32 (2)
C14'—C12'—C11'	108.06 (2)	C10—C9—C1	119.63 (2)
H12'—C12'—C13'	108.9 (2)	C8—C9—C1	122.086 (19)
H12'—C12'—C11'	107.5 (2)	C8—C9—C10	118.285 (19)
H12'—C12'—C14'	108.9 (2)	H14D—C14'—C12'	110.7 (3)
C12'—C11'—O1'	108.854 (18)	H14E—C14'—C12'	111.7 (2)
H11C—C11'—O1'	110.1 (2)	H14E—C14'—H14D	108.4 (4)
H11C—C11'—C12'	109.6 (2)	H14F—C14'—C12'	110.7 (3)
H11D—C11'—O1'	109.3 (2)	H14F—C14'—H14D	107.2 (4)
H11D—C11'—C12'	110.0 (2)	H14F—C14'—H14E	107.9 (4)
H11D—C11'—H11C	109.0 (3)	C4'—C3'—C2'	119.81 (2)
C1'—C2'—O1'	116.352 (17)	H3'—C3'—C2'	121.0 (2)
C3'—C2'—O1'	122.466 (19)	H3'—C3'—C4'	119.2 (2)
C3'—C2'—C1'	121.164 (19)	C10'—C4'—C3'	121.12 (2)
C1—C1'—C2'	119.137 (17)	H4'—C4'—C3'	119.5 (3)
C9'—C1'—C2'	119.204 (18)	H4'—C4'—C10'	119.3 (3)
C9'—C1'—C1	121.659 (18)	C5'—C10'—C4'	121.51 (2)
C2—C1—C1'	120.070 (17)	C9'—C10'—C4'	118.988 (19)
C9—C1—C1'	120.620 (18)	C9'—C10'—C5'	119.50 (2)
C9—C1—C2	119.275 (18)	C6'—C5'—C10'	120.86 (2)

C1—C2—O1	116.325 (17)	H5'—C5'—C10'	118.3 (3)
C3—C2—O1	122.572 (19)	H5'—C5'—C6'	120.8 (3)
C3—C2—C1	121.080 (19)	C7'—C6'—C5'	119.85 (2)
C12—C11—O1	108.047 (18)	H6'—C6'—C5'	121.1 (3)
H11A—C11—O1	110.0 (2)	H6'—C6'—C7'	119.0 (3)
H11A—C11—C12	110.3 (2)	C8'—C7'—C6'	120.57 (3)
H11B—C11—O1	109.6 (2)	H7'—C7'—C6'	119.8 (2)
H11B—C11—C12	110.6 (2)	H7'—C7'—C8'	119.7 (3)
H11B—C11—H11A	108.3 (3)	C9'—C8'—C7'	120.97 (2)
C13—C12—C11	111.71 (2)	H8'—C8'—C7'	120.6 (2)
C14—C12—C11	108.91 (2)	H8'—C8'—C9'	118.4 (2)
C14—C12—C13	111.60 (2)	C10'—C9'—C1'	119.71 (2)
H12—C12—C11	106.7 (2)	C8'—C9'—C1'	122.050 (19)
H12—C12—C13	109.0 (2)	C8'—C9'—C10'	118.242 (19)
H12—C12—C14	108.7 (2)	C7—C8—C9	120.98 (2)
H13A—C13—C12	111.7 (3)	H8—C8—C9	118.6 (2)
H13B—C13—C12	111.3 (3)	H8—C8—C7	120.4 (2)
H13B—C13—H13A	108.4 (4)	C6—C7—C8	120.51 (3)
H13C—C13—C12	110.4 (3)	H7—C7—C8	120.0 (2)
H13C—C13—H13A	106.7 (4)	H7—C7—C6	119.5 (2)
H13C—C13—H13B	108.1 (4)	C5—C6—C7	119.79 (2)
H14A—C14—C12	109.9 (3)	H6—C6—C7	119.6 (3)
H14B—C14—C12	111.1 (3)	H6—C6—C5	120.6 (3)
H14B—C14—H14A	107.3 (4)	C6—C5—C10	121.04 (2)
H14C—C14—C12	111.6 (3)	H5—C5—C10	118.5 (3)
H14C—C14—H14A	108.0 (4)	H5—C5—C6	120.5 (3)
O1'—C11'—C12'—C13'	60.63 (2)	C1—C2—C3—C4	2.26 (3)
O1'—C11'—C12'—C14'	−176.40 (2)	C1—C9—C10—C4	3.02 (2)
O1'—C2'—C1'—C1	−2.31 (2)	C1—C9—C10—C5	−176.67 (2)
O1'—C2'—C1'—C9'	177.507 (17)	C1—C9—C8—C7	177.56 (2)
O1'—C2'—C3'—C4'	−177.60 (2)	C2—C3—C4—C10	−1.58 (3)
O1—C2—C1—C1'	0.17 (2)	C3—C4—C10—C9	−1.05 (3)
O1—C2—C1—C9	178.054 (19)	C3—C4—C10—C5	178.64 (2)
O1—C2—C3—C4	−175.95 (2)	C4—C10—C9—C8	−177.27 (2)
O1—C11—C12—C13	62.99 (2)	C4—C10—C5—C6	178.65 (3)
O1—C11—C12—C14	−173.29 (2)	C10—C9—C8—C7	−2.14 (3)
C2'—C1'—C1—C2	109.31 (2)	C10—C5—C6—C7	−0.70 (3)
C2'—C1'—C1—C9	−68.54 (2)	C9—C8—C7—C6	−0.21 (3)
C2'—C1'—C9'—C10'	0.44 (2)	C3'—C4'—C10'—C5'	178.96 (2)
C2'—C1'—C9'—C8'	−179.856 (19)	C3'—C4'—C10'—C9'	−0.49 (3)
C2'—C3'—C4'—C10'	−0.05 (3)	C4'—C10'—C5'—C6'	179.95 (2)
C1'—C1—C2—C3	−178.14 (2)	C4'—C10'—C9'—C8'	−179.43 (2)
C1'—C1—C9—C10	175.502 (19)	C10'—C5'—C6'—C7'	−0.19 (3)
C1'—C1—C9—C8	−4.19 (2)	C10'—C9'—C8'—C7'	−0.86 (2)
C1'—C9'—C10'—C4'	0.29 (2)	C5'—C6'—C7'—C8'	0.46 (3)
C1'—C9'—C10'—C5'	−179.17 (2)	C6'—C7'—C8'—C9'	0.08 (3)
C1'—C9'—C8'—C7'	179.43 (2)	C8—C7—C6—C5	1.66 (3)

Hydrogen-bond geometry (Å, °)

Cg1 and *Cg2* are the centroids of the C5–C10 and C5'–C10' rings, respectively.

<i>D</i> —H··· <i>A</i>	<i>D</i> —H	H··· <i>A</i>	<i>D</i> ··· <i>A</i>	<i>D</i> —H··· <i>A</i>
C13—H13 <i>A</i> ··· <i>Cg2</i>	1.091 (4)	2.998 (5)	4.0338 (4)	158.7 (3)
C13'—H13 <i>E</i> ··· <i>Cg1</i>	1.091 (5)	2.877 (5)	3.8615 (4)	150.1 (3)
C13—H13 <i>C</i> ··· <i>Cg2</i> ⁱ	1.083 (5)	2.987 (5)	3.6455 (4)	119.6 (3)

Symmetry code: (i) $x, -y+3/2, z+1/2$.